THE JOURNAL OF BIOLOGICAL CHEMISTRY VOL. 290, NO. 12, pp. 7426–7435, March 20, 2015

Intracellular Screening of a Peptide Library to Derive a Potent Peptide Inhibitor of α-Synuclein Aggregation*

Received for publication, October 21, 2014, and in revised form, January 12, 2015 Published, JBC Papers in Press, January 23, 2015, DOI 10.1074/jbc.M114.620484

Harish Cheruvara[‡], Victoria L. Allen-Baume[‡], Neil M. Kad[§1], and Jody M. Mason[¶1,2]

From the [‡]School of Biological Sciences, University of Essex, Wivenhoe Park, Colchester, Essex CO4 3SQ, the [§]School of Biosciences, University of Kent, Canterbury, Kent CT2 7NJ, and the [¶]Department of Biology and Biochemistry, University of Bath, Claverton Down, Bath BA2 7AY, United Kingdom

Background: Deposition of α-synuclein into Lewy bodies is considered the primary event in Parkinson disease.
Results: A peptide selected via PCA library screening functions by inhibiting fibril formation.
Conclusion: A semirational design combined with intracellular PCA is an effective methodology to develop α-synuclein aggregation antagonists.
Significance: The technique can be applied to a number of diseases from Parkinson to Alzheimer.

Aggregation of α-synuclein (α-syn) into toxic fibrils is a pathogenic hallmark of Parkinson disease (PD). Studies have focused largely on residues 71–82, yet most early-onset mutations are located between residues 46 and 53. A semirationally designed 209,952-member library based entirely on this region was constructed, containing all wild-type residues and changes associated with early-onset PD. Intracellular cell survival screening and growth competition isolated a 10-residue peptide antagonist that potently inhibits α-syn aggregation and associated toxicity at a 1:1 stoichiometry. This was verified using continuous growth measurements and 3-(4,5-dimethylthiazol-2-yl)-2,5-diphenyltetrazolium bromide cytotoxicity studies. Atomic force microscopy and circular dichroism on the same samples showed a random-coil structure and no oligomers. A new region of α-syn for inhibitor targeting has been highlighted, together with the approach of using a semirational design and intracellular screening. The peptides can then be used as candidates for modification in drugs capable of slowing or even preventing the onset of PD.

Deposition of α-synuclein (α-syn)[3] into neuronal inclusions known as Lewy bodies is considered the causative agent in the pathogenesis of Parkinson disease (PD), a debilitating disease that results principally in rigidity, tremor, and slowness of movement and that accounts for ~15% of all dementias (1, 2). The accumulation of toxic Lewy bodies in the cytoplasmic space of dopaminergic neurons in the substantia nigra pars compacta region of the brain leads to cell death, decreased dopamine levels, and ultimately the symptoms of the disease. There is a substantial and growing body of evidence implicating α-syn in PD (3), including (i) synthetic α-syn rapidly aggregates into β-sheet-rich fibrils similar to those found in Lewy bodies; (ii) rare familial mutations that increase fibril aggregation rates and toxicity lead to early-onset PD; (iii) α-syn gene duplications lead to increased protein expression and therefore accelerate disease onset; and (iv) α-syn oligomers are toxic to therapeutically relevant cells in culture. To intervene in PD, we utilized a novel intracellular screen to identify peptides capable of binding to and reducing the associated toxicity of a-syn aggregation. Our approach has the potential to address recent findings that suggest that prefibrillar oligomers are the toxic species (4).

There is a wealth of experimental data demonstrating that region 71–82 is responsible for aggregation of the full-length 140-amino acid protein (5–7). Indeed, numerous groups have used this region as a starting point for the design of inhibitors. This has included unmodified peptides (8) and *N*-methylated peptides (9). Given the interest in this region and its requirement for aggregation of the full-length protein, many groups have focused their efforts on producing libraries based on this scaffold. However, of the known point mutations in the α-syn gene associated with early-onset PD, three (E46K, H50Q, A53T) are located between residues 46 and 53, with the fourth (A30P) located in close proximity. More recently, a fifth mutation (G51D) was identified (10). This region and the residues within are clearly important in modulating amyloid formation such that toxicity associated with the α-syn protein increases, with the changes leading to decreased α-helicity, increased β-sheet propensity, and an increase in either the rate or number of oligomers that are formed (11–14).

In this study, we generated peptide inhibitors using a multiplexed intracellular protein-fragment complementation assay (PCA) library screening system (15, 16), followed by direct imaging of the samples. Successfully selected peptides must bind α-syn to reduce amyloid cytotoxicity and confer bacterial cell survival. During PCA, no assumptions are therefore made regarding the mechanism of action or the oligomeric state of α-syn that becomes populated. The only prerequisites for peptide selection are that (i) peptides bind to α-syn such that the split reporter enzyme is recombined and (ii) the result is lower

* This work was supported by Parkinson's UK Ph.D. Studentship H-1001 (to H. C., N. M. K., and J. M. M.) and by Cancer Research UK Career Establishment Award A11738 (to J. M. M.).
[1] Both authors contributed equally to this work.
[2] To whom correspondence should be addressed. E-mail: j.mason@bath.ac.uk.
[3] The abbreviations used are: α-syn, α-synuclein; PD, Parkinson disease; PCA, protein-fragment complementation assay; ThT, thioflavin T; AFM, atomic force microscopy; MTT, 3-(4,5-dimethylthiazol-2-yl)-2,5-diphenyltetrazolium bromide; SUMO, small ubiquitin-like modifier; Fmoc, *N*-(9-fluorenyl)methoxycarbonyl.

toxicity such that cell survival is facilitated. In addition, the PCA approach is predicted to select peptides that are resistant to degradation by bacterial proteases, soluble, nontoxic, and target-specific in the presence of other cytoplasmic proteins.

Using α-syn(45–54) as a template for our library design, we created a 209,952-member peptide library 10 amino acids in length that spans residues 45–54, containing the wild-type 45–54 sequence, including residue options corresponding to E46K, H50Q, and A53T, which, when mutated, give rise to early-onset PD. PCA was used to screen the peptide library for an interaction with wild-type α-syn. The effectiveness of an amyloid/PCA-selected peptide (45–54W) was subsequently tested by performing four key experiments upon the same sample: a continuous amyloid growth assay, monitored using thioflavin T (ThT) fluorescence; CD, to report on changes in β-sheet content; and atomic force microscopy (AFM) and SDS-PAGE analysis, to directly image any reduction in fibril load and changes in the fibril morphology. We found the peptide derived using this approach to be capable of binding to the disease-relevant wild-type α-syn and reducing associated amyloid formation by >90%. In this study, we both successfully verified the methodology for producing anti-α-syn aggregation peptide inhibitors using the amyloid/PCA approach and produced a lead peptide sequence that is expected to provide a scaffold for future drug candidates.

Our data collectively indicate that the PCA-derived winner sequence (45–54W) is able to prevent the aggregation of wild-type α-syn at a stoichiometry of 1:1. The ThT fluorescence signal associated with amyloid formation did not progress beyond ~8% of the original 1:0 sample. AFM experiments showed that in the same continuous growth samples, there was a striking decrease in the number of fibrils relative to the 1:0 samples. 3-(4,5-Dimethylthiazol-2-yl)-2,5-diphenyltetrazolium bromide (MTT) cytotoxicity studies using the same samples showed a reduction in cell death of 65–85% compared with α-syn in isolation. Finally, CD experiments using samples taken from the same continuous growth experiment once again showed that the conversion from a random-coil structure to a β-sheet-rich structure was almost completely abolished in the 1:1 sample. At a molar ratio of 1:0.5, the formation of the mature amyloid fibrils found in the 1:0 sample was slowed but ultimately not prevented (see Fig. 3*a*). At stoichiometries of 1:0.1 and 1:0.01, the rate of amyloidosis was not significantly lowered relative to the 1:0 sample.

EXPERIMENTAL PROCEDURES

Primers and Library Cloning—Primers were designed such that the desired library could be generated using overlap-extension PCR. Bases overlapped in a non-randomized region of the primers to give an approximate annealing temperature of 66 °C. Correct amplification was enabled via an elongated reverse primer and verified by agarose gel electrophoresis. The correct PCR product was then digested using NheI and AscI restriction enzymes for subcloning the library into the pES230d vector (restriction enzyme recognition sites shown). Primer sequences used were 5′-C TGG GCT AGC RAA VAW GBG VTT VTT VAW GBG VTT RHA RCC GGC GCG CCG CTA GAG GCG-3′ (forward) and 5′-T TTT TTT TTA TAA TAT ATT ATA CGC CTC TAG CGG CGC GCC-3′ (reverse). An additional 30 residues on the 5′-end of the reverse primer were used to observe the correct PCR product prior to restriction digestion.

Single-step Selection PCA—Escherichia coli XL-1 cells were used for construction and cloning of libraries as described previously (16–18). First, pES300d-α-syn target and pREP4 (for expression of the Lac repressor protein; Qiagen) were cotransformed into BL21-Gold cells (Stratagene) and plated onto LB agar with the appropriate antibiotics (kanamycin and chloramphenicol). These cells were next made electrocompetent before transformation with the pES230d-45–54 library plasmid. Transformed cells were plated onto three different media. One-twentieth of the cells were plated onto LB agar with three antibiotics (kanamycin, ampicillin, and chloramphenicol) as a positive control of transformation efficiency. Another one-twentieth of the solution was plated onto M9 minimal agar containing 1 μg/ml trimethoprim and the same three antibiotics as a negative control. Finally, the remaining 90% of the transformed cells were plated onto M9 minimal agar in the presence of the three antibiotics, 1 μg/ml trimethoprim, and 1 mM isopropyl β-D-thiogalactopyranoside to induce expression of the two dihydrofolate reductase fragment-fused peptides. This single-step selection PCA led to ~200 colonies from the initial library of 209,952, meaning that >99.9% of all library members were removed at this stage.

Competition Selection PCA—To increase selection stringency, growth competition experiments were undertaken. Selected colonies were pooled from the plate, grown in M9 minimal agar under selective conditions (containing kanamycin, ampicillin, chloramphenicol, trimethoprim, and isopropyl β-D-thiogalactopyranoside), and serially diluted over five passages. Using these sequential rounds of competition selection, subtle differences in growth rate can become amplified, increasing the stringency of selection relative to the single-step method. Competition selection therefore allows the most effective one or two sequences to be isolated from the ~200 α-syn binders initially identified during single-step selection. At each passage, glycerol stocks were prepared, and sequencing results were obtained (Source Bioscience, Nottingham, United Kingdom) for DNA pools and individual colonies. For each passage, 50 μl of liquid culture was added to 50 ml of fresh M9 minimal agar, resulting in an A_{600} of ~0.01. Cells were incubated at 37 °C until an A_{600} of ~0.4 was reached (typically 2–3 days) before moving to the next passage.

Protein Expression and Purification—Wild-type α-syn was synthesized by overexpression in the *E. coli* BL21 strain using a small ubiquitin-like modifier (SUMO) fusion protein (19). SUMO modulates protein structure and function by covalently binding to the lysine side chains of the target protein to enhance expression and solubility of the α-syn protein. *E. coli* BL21 competent cells were transformed with the pET21b plasmid construct, grown on LB agar plates containing ampicillin and chloramphenicol, and grown overnight. Single colonies were next picked, inoculated in LB broth containing ampicillin and chloramphenicol, and shaken at 37 °C. These cultures were then used to inoculate 2 liters of liquid LB broth containing ampicillin and chloramphenicol and grown to mid-log phase (A_{600} = 0.6–0.8) before being further induced by 1 mM isopro-

pyl β-D-thiogalactopyranoside for 3 h at 37 °C. Cells were obtained by centrifugation at 4000 rpm for 20 min at 4 °C in a Sorvall RC Superspeed centrifuge. Cell pellets were then resuspended in binding buffer (50 mM NaH_2PO_4, 300 mM NaCl, and 10 mM imidazole (pH 8)) and homogenized using a magnetic stirrer for 15 min on ice, followed by sonication (40% amplification). Lysed cells were next centrifuged at 18,500 rpm for 20 min at 4 °C using an SS-34 rotor (Sorvall RC Superspeed centrifuge). The supernatant containing the protein was stored at −20 °C.

The fusion protein was purified by applying the supernatant from the cell lysate to a nickel-nitrilotriacetic acid affinity column three times at a flow rate of 3 ml/min to allow the protein to bind. The column was next washed with 40 ml of wash buffer (50 mM NaH_2PO_4, 300 mM NaCl, and 30 mM imidazole (pH 8)), and the protein was eluted using elution buffer (50 mM NaH_2PO_4, 300 mM NaCl, and 500 mM imidazole (pH 8)). The protein sample was then exchanged to cleavage buffer (20 mM Tris and 0.5 mM DTT (pH 8)) using a PD-10 desalting column. The His_6-SUMO tag was removed using the SUMO protease-specific UlP1 enzyme (1 mg/ml for 10 mg/ml target protein) at 30 °C for 16 h.

His_6-SUMO was finally removed using a size-exclusion column. A Sephadex G-75 column was washed three times with 10 mM MES and 150 mM NaCl (pH 8.0). The protein was concentrated to 2 ml and injected onto the column, and fractions were eluted according to their molecular mass. Finally, SDS-PAGE was used to determine the purity of the α-syn and to verify the expected molecular mass of different fractions containing α-syn (14.5 kDa), SUMO protein (12.2 kDa), and SUMO protease (27 kDa). The correct mass of α-syn was further confirmed by electrospray mass spectrometry. The protein concentration was determined in a Varian Cary 50 spectrophotometer. The purified protein was lyophilized using a freeze drier and stored at −80 °C.

Monomerization of Protein for Aggregation Studies—To monomerize the protein prior to aggregation experiments, 1 ml of hexafluoro-2-propanol was added to 2 mg of lyophilized peptide. This was next vortexed for ~2 min to fully dissolve the peptide, followed by sonication at 25 °C for 5 min in a water bath sonicator. Hexafluoro-2-propanol was allowed to evaporate completely under a regulated stream of air. The process was repeated three times, followed by dissolution of the peptide sample in double-distilled water, vortexing for 3 min, and lyophilization for further use (9).

Peptide Synthesis—Rink amide ChemMatrix resin was obtained from PCAS BioMatrix Inc. (Saint-Jean-sur-Richelieu, Quebec, Canada). Fmoc-L-amino acids and (1*H*-benzotriazol-1-yloxy)-(dimethylamino)-*N*,*N*-dimethylmethaniminium hexafluorophosphate were obtained from AGTC Bioproducts (Hessle, United Kingdom). All other reagents were of peptide synthesis grade and obtained from Thermo Fisher Scientific (Loughborough, United Kingdom). Peptide 45–54W was synthesized on a 0.1-mmol scale on PCAS BioMatrix Rink amide resin using a Liberty Blue microwave peptide synthesizer (CEM Corp., Matthews, NC) employing Fmoc solid-phase techniques (for review, see Ref. 20) with repeated steps of coupling, deprotection, and washing (4× 5 ml of dimethylformamide). Coupling was performed as follows: Fmoc-L-amino acids (5 eq), (1*H*-benzotriazol-1-yloxy)(dimethylamino)-*N*,*N*-dimethylmethaniminium hexafluorophosphate (4.5 eq), and diisopropylethylamine (10 eq) in dimethylformamide (5 ml) for 5 min with 20-watt microwave irradiation at 90 °C. Deprotection was performed as follows: 20% piperidine in dimethylformamide for 5 min with 20-watt microwave irradiation at 80 °C. Following synthesis, the peptide was acetylated (acetic anhydride (3 eq) and diisopropylethylamine (4.5 eq) in dimethylformamide (2.63 ml) for 20 min) and then cleaved from the resin with concomitant removal of side chain-protecting groups by treatment with a cleavage mixture (10 ml) consisting of TFA (95%), triisopropylsilane (2.5%), and H_2O (2.5%) for 4 h at room temperature. Suspended resin was removed by filtration, and the peptide was washed by three rounds of crashing in ice-cold diethyl ether, vortexing, and centrifugation. The pellet was then dissolved in 1:1 MeCN/H_2O and freeze-dried. Purification was performed by reverse-phase HPLC using a Phenomenex Jupiter Proteo (C12) reverse-phase column (4 μm, 90 Å, 10 mm, inner diameter × 250 mm long). Eluents used were as follows: 0.1% TFA in H_2O (eluent A) and 0.1% TFA in MeCN (eluent B). The peptide was eluted by applying a linear gradient (at 3 ml/min) of 20–60% eluent B over 40 min. Fractions collected were examined by electrospray mass spectrometry, and those found to contain the desired product exclusively were pooled and lyophilized. Analysis of the purified final product by reverse-phase HPLC indicated a purity of >95%.

Peptide Preparation—Stock solutions of 1 mM inhibitor and control peptides were dissolved in ultrapure water. At this concentration (a 2–200-fold excess of that used in experiments), no aggregation or precipitation was observed. In addition, bioinformatics tools (*e.g.* Waltz (21), AmylPred (22), PASTA (23), Zyggregator (24), and TANGO (25)) did not predict the peptide to contain amyloidogenic sequences or to aggregate in isolation. Finally, dye-binding experiments demonstrated that this sequence did not bind ThT or aggregate and form random coil-like species in isolation by CD (see Figs. 3 and 4).

Continuous Growth ThT Experiments—Peptides were lyophilized at the molar concentration of the target protein and inhibitory peptide (1:1). The reaction mixture containing 450 μM wild-type α-syn and inhibitory peptide was incubated in 90 μM ThT, 10 mM phosphate buffer (pH 7.0), 100 mM KF, and 0.05% NaN_3 at 37 °C with continuous mixing using a magnetic stir bar in an LS 55 fluorescence spectrophotometer (Perkin-Elmer Life Sciences) for 4500 min (75 h). The same experiment was repeated three times for both the 1:0 sample- and peptide 45–54W-containing solutions at a variety of stoichiometries, as well as at 1:1 molar ratios with the wild-type 45–54 and 71–82W (Ac-VTGVTADVQETV-NH2) control peptides. The PCA winner peptide, 45–54W, was lyophilized in aliquots of different molar concentrations of target protein and inhibitory peptide ranging from 1:0.01 to 1:1.

CD Experiments—Far-UV CD spectra were recorded using an Applied Photophysics Chirascan spectrometer at 20 °C using the same samples from the continuous growth ThT experiments. Spectra were recorded over the 190–300-nm range at a scan rate of 10 nm/min with step size of 1 nm. Spectra were recorded as the average of three scans. Peptide (10 μM in 10 mM potassium phosphate buffer (pH 7.4)) was added to a

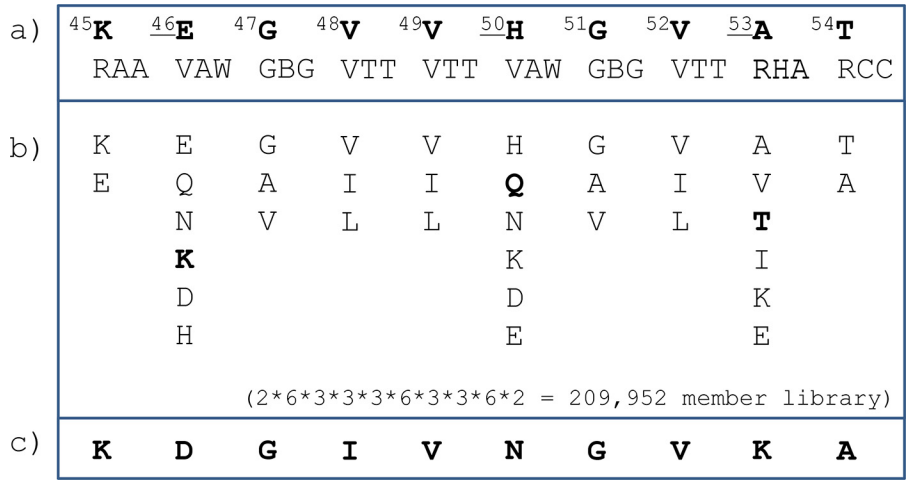

FIGURE 1. *a*, shown are residues 45–54 of wild-type α-syn (KEGVVHGVAT), as well as the three well studied point mutation sites (positions 46, 50, and 53). Degenerate codons for library construction are shown below (*R* = A/G, *V* = A/C/G, *W* = A/T, *B* = C/G/T, and *H* = A/C/T). *b*, shown are amino acid options at each position to generate a 209,952-member peptide library. The wild-type residue options (top line) and alternative options, including those point mutations associated with early-onset PD (shown in *boldface*), were also considered in the library design. *c*, the PCA winner peptide (KDGIVNGVKA) emerged from single-step selection, followed by two rounds of competition selection PCA.

0.1-cm cuvette (Hellma Analytics). Spectra were recorded as raw ellipticity.

AFM Experiments—Samples were imaged in noncontact mode using an XE-120 atomic force microscope (Park Systems, Suwon, South Korea). NSC15 silicon nitride cantilevers with a spring constant of 40 newtons/m were used for imaging at a scan rate of 1.0 Hz and a resolution of 256 × 256 pixels. All images were obtained at room temperature. The AFM data were taken from continuous growth experiments. A 5-μl sample was taken from the 450 μM α-syn continuous growth experiment and placed on freshly cleaved mica (0.3-mm thickness). Following adsorption of the protein aggregates (2 min), the mica was washed with 5 ml of double-distilled water. Excess water was removed, and the samples were dried using a stream of nitrogen gas. Samples were immediately analyzed by AFM. The image files were examined using WSxM 5.0 (Nanotec Electronica S.L.) and flattened before processing (26).

MTT Cell Toxicity Assay—MTT experiments were undertaken using rat pheochromocytoma (PC12) cells to assess the cytotoxicity effect of α-syn. PC12 cells are known to be particularly sensitive, and their use in this assay is well established (27). A Vybrant MTT cell proliferation assay kit (Invitrogen) was used to measure conversion of the water-soluble MTT dye to formazan, which was then solubilized, and the concentration was determined by a purple color change monitored via absorbance measurement at 570 nm. The change in absorbance can be used as an indicator of PC12 cell health in this assay. The assay was performed with a 5 μM α-syn and peptide stoichiometry corresponding to 1:1. PC12 cells were maintained in RPMI 1640 medium and 2 mM glutamine mixed with 10% horse serum and 5% fetal bovine serum and supplemented with 20 mg/ml gentamycin. Cells were transferred to a sterile 96-well plate with 30,000 cells/well, and experiments were performed in triplicate. The required volume of peptide and target solutions was added to PC12 cells. A total of 100 μl of PC12/RPMI 1640 medium combined with an appropriate volume of peptide/α-syn target mixture (5 μM peptide + 5 μM α-syn target) was transferred to a 96-well microtiter plate. Because the samples contained 90 μM ThT, control experiments with PC12 cells and α-syn alone both with and without ThT were undertaken. These samples were incubated for 24 h at 37 °C and 5% CO_2 prior to the addition of the MTT dye. A total of 10 μl of the dye was added to each well and incubated for an additional 4 h at 37 °C and 5% CO_2. A total of 100 μl of dimethyl sulfoxide was then added to each well and allowed to stand for 10 min. The absorbance was measured at 570 nm using a Berthold TriStar LB 942 plate reader.

SDS-PAGE—Gel analysis was carried out using 15% Tris bisacrylamide gels operated at a constant voltage of 150 V. The running buffer was 25 mM Tris-HCl, 193 mM glycine, and 0.1% SDS (pH 8.3). 3 μl of 450 μM α-syn and peptides at different stoichiometries was mixed with 7 μl of loading buffer containing 50 mM Tris-HCl (pH 6.8), 1% SDS, 5% glycerol, and 25% bromphenol blue. 10 μl of each sample was then loaded in each well. The gel was stained with 0.1% Coomassie Blue R-250.

RESULTS

α-syn(45–54) Library Generation—PCA was undertaken with the full-length α-syn(1–140) target using a library based on the α-syn(45–54) region, in which three of the four α-syn mutations associated with early-onset PD are located (KEGVVHGVAT, wild-type 45–54). Unlike α-syn(71–82), this is not a region of the molecule known to aggregate into toxic fibrils in isolation (28–30) and therefore has not been exploited as a starting point for deriving α-syn binders capable of inhibiting aggregation. The library incorporated the wild-type sequence while introducing two-, three-, or six-residue options at each of the 10 amino acid positions (Fig. 1). This corresponded to a library size of 209,952. Single-step selection on M9 plates was undertaken, followed by competition selection in liquid M9 medium, resulting in one clean sequencing result by passage 6: KDGIVNGVKA (Fig. 2).

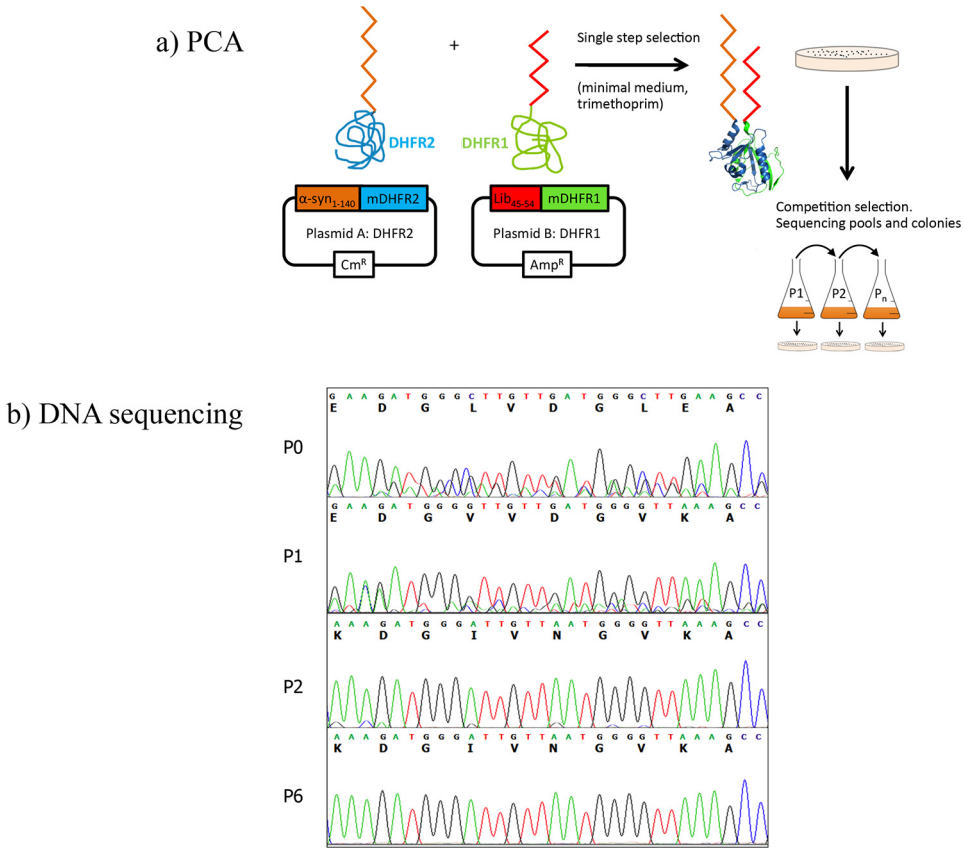

FIGURE 2. *a*, PCA. Peptide library members that bind to wild-type α-syn(1–140) recombine murine dihydrofolate reductase (*mDHFR*) and lead to colonies under selective conditions (bacterial dihydrofolate reductase is specifically inhibited using trimethoprim). Those peptides that bind with the highest affinity to the α-syn target are able to confer cell growth by (i) reconstituting murine dihydrofolate reductase to restore activity and (ii) reducing the toxicity associated with any given oligomeric amyloid state. In competition selection, subsequent passages in liquid medium isolate potential PCA winners with the highest efficacy. Because PCA is performed in the cytoplasm of *E. coli*, the nonspecific, unstable, aggregation-prone (insoluble), protease-susceptible members are removed. *b*, DNA sequencing results of library pools for passages 0–6. Both single-step selection (*P0*) and competition selection (*P1*, *P2*, and *P6*) are shown. The peptide sequence KDGIVNGVKA was seen to dominate from passage 2 onwards. Cm^R, chloramphenicol resistance; Amp^R, ampicillin resistance.

Peptide Characterization—PCA-derived peptide sequences (Fig. 1) were synthesized and characterized using a number of experiments, including ThT dye binding, CD, AFM, and MTT cytotoxicity experiments, to verify that the peptides do not aggregate in isolation and to determine whether they are able to reduce aggregation and/or breakdown preformed fibrils to a nontoxic species.

Continuous Growth ThT Experiments Demonstrate a Significant Reduction in Fibril Load—To determine the ability of PCA-derived peptides to reduce fibril assembly (inhibition) and/or to breakdown preformed fibrils (reversal), ThT binding was used to quantify amyloid species. First, α-syn was rendered monomeric (9) and aggregated into amyloid by resuspending and incubating at 37 °C. For the continuous growth assay, peptides were added at time 0, and a reading was taken every 5 min over a 75 h period. The ThT signal was significantly reduced at a 1:1 molar ratio, indicating that the peptides were able to bind α-syn and reduce aggregation levels. At increasingly lower substoichiometric ratios, we observed progressively reduced activity consistent with a general dose dependence. The control peptide 71–82W and the wild-type 45–54 sequence at 1:1 molar rations had no effect on aggregation, demonstrating α-syn specificity for peptide 45–54W.

AFM Indicates a Large Reduction in Amyloid Levels—As a second direct qualitative measure of fibril formation, samples used in continuous growth experiments were imaged using AFM (Fig. 3, *b–f*). A stoichiometry of 1:1 (450 μM) was chosen for AFM experiments, as this was found to be the most effective in ThT experiments (Fig. 3*b*). At this stoichiometry, a major reduction in the amount of amyloid was observed relative to the α-syn control across several time points (Fig. 3*d*). No fibrils were observed for peptide 45–54W in the absence of α-syn. The control peptide 71–82W and the wild-type 45–54 sequence had no effect upon fibril formation (Fig. 3, *e* and *f*), supporting α-syn specificity for peptide 45–54W.

CD Demonstrates a Large Reduction in β-Sheet Content—Because amyloid fibrils are predominately β-sheet, we also used CD spectroscopy for structural characterization of the aggregates in the continuous growth ThT experiments. The data presented in Fig. 4*a* show spectra over 17 time points of the continuous growth assay. A single negative peak at 218 nm develops across the time course, along with the loss of the minimum at ~200 nm, consistent with the gain of β-sheet structure and the loss of a random coil. As predicted from the ThT data above, the β-structure did not form for α-syn incubated with peptide 45–54W at a 1:1 stoichiometry (Fig. 4*b*). In addition, the minimum at ~200 nm did not significantly diminish. A similar spectrum was observed for peptide 45–54W alone (*i.e.* 0:1 stoichiometry) after 75 h of incubation, indicating that this peptide does not aggregate in isolation. The lack of CD signal

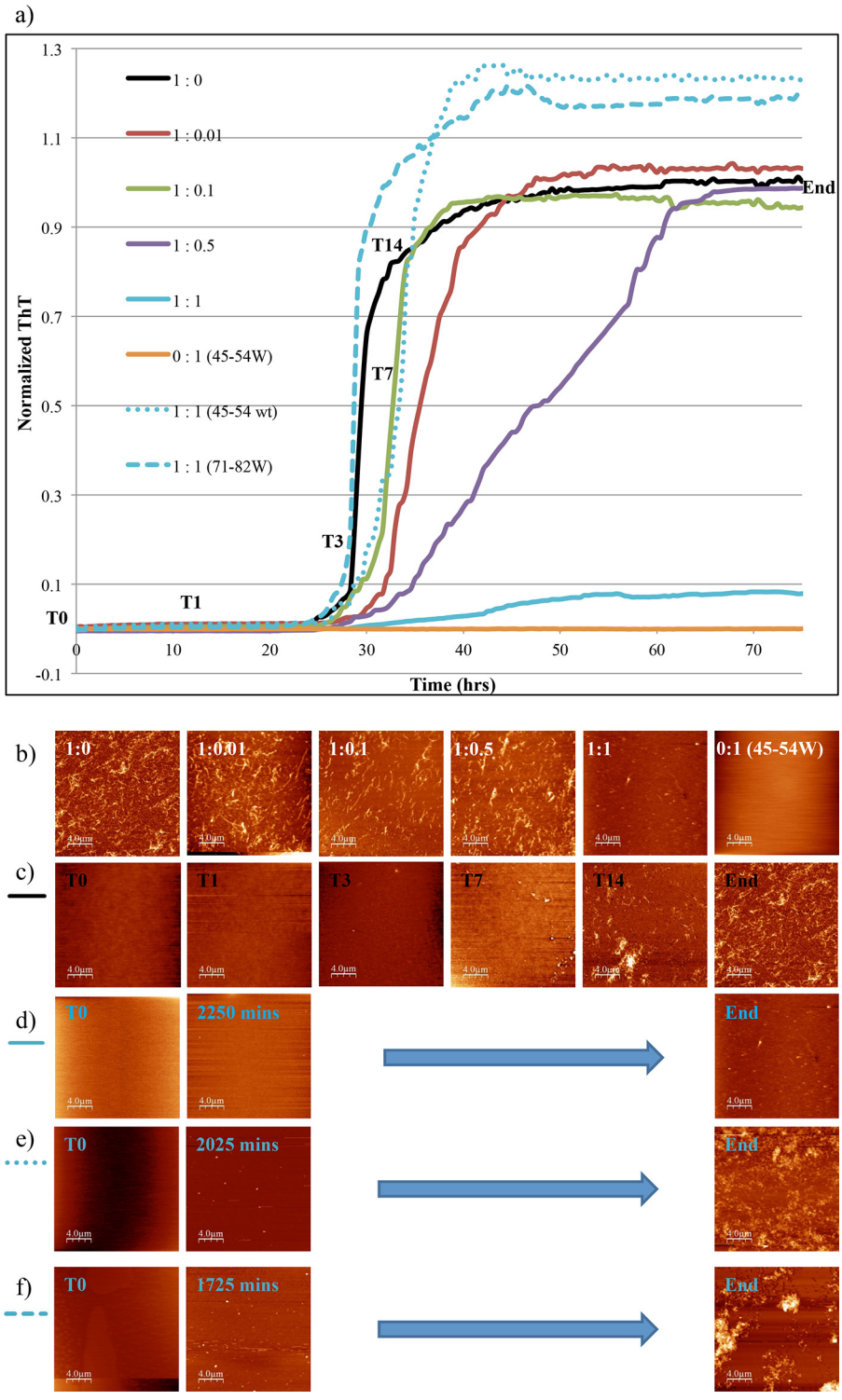

FIGURE 3. *a*, continuous ThT growth. The data show a significant reduction in ThT signal (~92%) at a 1:1 stoichiometry. The ThT signal at a molar ratio of 1:0.5 shows that the amyloid growth rate was significantly reduced compared with the wild type. At increasingly substoichiometric ratios, the ThT fluorescence indicates reduced peptide activity in an expected dose-dependent manner. Peptide 45–54W alone (0:1 sample) showed no ThT binding, indicating that it does not aggregate in isolation. Aliquots of samples were collected at 17 different time points for the 1:0 sample (lag phase (*T0* and *T1*), exponential phase (*T3*, *T7*, and *T14*), and stationary phase (*End*) are shown) and three time points for the 1:1 sample (*T0*, *T1*, and *End*) for further analysis by AFM and CD. *b*, AFM images showing the end point samples (75 h) for all stoichiometries used in continuous growth ThT experiments. A considerable reduction in fibril load was observed at a molar ratio of 1:1. All other stoichiometries showed no major reduction in amyloid content relative to the 1:0 sample. Peptide 45–54W (0:1 sample) did not aggregate in isolation. *c*, AFM images showing the gradual increase in amyloid content along various time points for the 1:0 sample. Shown are six samples (*T0*, *T1*, *T3*, *T7*, *T14*, and *End*) taken from the lag, exponential, and stationary phases. The time points for these were 0, 10, 33.3, 37.5, 49, and 75 h, respectively. *d*, a large reduction in amyloid content was observed for the 1:1 sample with peptide 45–54W. For these images, $T0 = 0$ h, $T1 = 37.5$ h, and $T2 = 75$ h. *e*, no reduction in amyloid content was observed for the 1:1 sample with the wild-type 45–54 sequence. For these images, $T0 = 0$ h, $T1 = 33.75$ h, and $T2 = 75$ h. *f*, no reduction in amyloid content was observed for the 1:1 sample with peptide 71–82W. For these images, $T0 = 0$ h, $T1 = 28.75$ h, and $T2 = 75$ h. For all samples, many images were taken at each time point to confirm the morphology and number of fibrils present in each image.

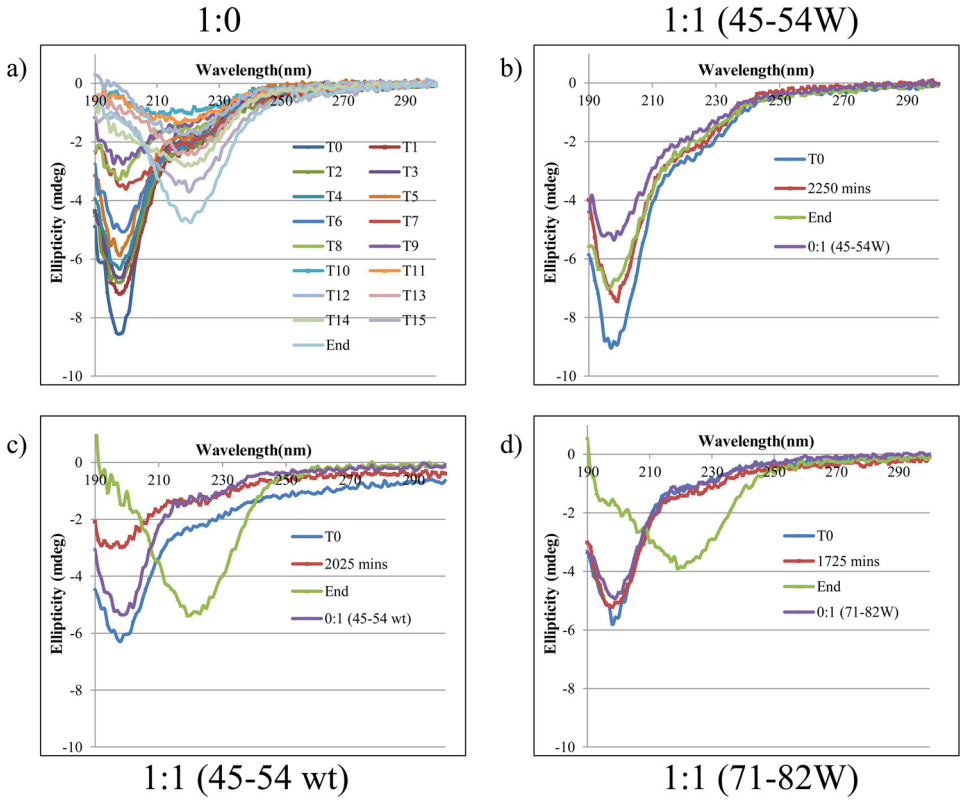

FIGURE 4. *a*, CD spectra of the same samples used in the ThT and AFM experiments. Shown is the gradual development of a minimum at 218 nm across the time course along with the loss of a minimum at 200 nm, consistent with the gain of β-sheet structure and the loss of a random coil in the 1:0 sample. *b*, in the 1:1 samples, the minimum at ~200 nm was prominent even after 75 h of incubation, with no development of a 218 nm signal, confirming the efficacy of peptide 45–54W in preventing the formation of β-sheet structure. A similar spectrum was obtained for peptide 45–54W (0:1 samples), confirming that the peptide does not adopt a β-sheet structure in isolation. *c*, a 1:1 sample with the wild-type 45–54 sequence had no effect upon conversion to the β-sheet structure and loss of a random coil. The wild-type 45–54 sequence in isolation (0:1 samples) did not adopt a β-sheet structure in isolation. *d*, similarly, a PCA-derived peptide based on region 71–82 of α-syn had no effect upon conversion to β-sheet structure and loss of a random coil. Again peptide 71–82W in isolation (0:1 samples) did not adopt a β-sheet structure in isolation. *mdeg*, millidegrees.

intensity at 218 nm for α-syn incubated with peptide 45–54W is unlikely to be attributed to increased aggregation or precipitation. This is because any peptides causing increased precipitation would also generate large increases in ThT binding and would be clearly observed in AFM imaging experiments. Neither wild-type α-syn(45–54) nor peptide 71–82W had any effect upon conversion to the β-structure (Fig. 4, *c* and *d*), again demonstrating α-syn specificity for peptide 45–54W.

MTT Studies Demonstrate Reduced Amyloid Toxicity of Cells—MTT cell toxicity experiments were performed using rat pheochromocytoma (PC12) neuron-like cells to assess the toxicity of α-syn and the preventative effects of peptide 45–54W generated in this study. MTT assays were performed at a α-syn/peptide 45–54W ratio of 1:1 and are presented as raw A_{570} signal (Fig. 5*a*). At this stoichiometry, peptide 45–54W improved cell viability by 65–85% relative to α-syn in isolation. Dose dependence experiments demonstrated that at molar ratios of 1:0.01 and 1:0.1, there was no effect on toxicity. At 1:0.5, the recovery was improved, maximizing at 1:1 and becoming less pronounced at increasingly higher molar ratios (Fig. 5*b*). In addition, MTT experiments using samples taken throughout the continuous growth experiment demonstrated that α-syn became progressively more toxic with time and was most toxic within the stationary phase of fibril growth (Fig. 5*c*). As predicted from ThT, CD, and AFM experiments, MTT experiments using the wild-type 45–54 sequence or peptide 71–82W demonstrated that although these peptides were not toxic in isolation, they had very little effect on α-syn toxicity (Fig. 5*d*). Finally, increasing the concentrations of peptide 45–54W in isolation demonstrated that it was not toxic.

SDS-PAGE Analysis Demonstrates that Peptide 45–54W Is Able to Interact with α-syn and Lower the Oligomeric State—A range of samples were taken from the end point (75 h) of the continuous growth experiments and subjected to SDS-PAGE analysis (Fig. 6). Two clear bands at ~40 and ~60 kDa (as determined by graph analysis of log molecular mass *versus* relative migration distance; data not shown) were found to be present in the 1:0 sample, as well as in the 1:0.01, 1:0.1, and 1:2 samples and, to a lesser extent, the 1:5 sample, suggesting the presence of α-syn trimers (40/14.5 = 2.8) and tetramers (60/14.5 = 4.1). No bands corresponding to dimers or 5–8-mers were observed. At a molar ratio of 1:1 or higher, these bands were found to absent and were replaced with three low molecular mass bands. One band at ~15 kDa may represent the α-syn·peptide 45–54W complex. The second and third bands are below the resolution limit of the gel but are likely to represent monomeric α-syn (14.5 kDa) and the inhibitor alone (1 kDa). Although under denaturing conditions (therefore precluding more detailed interpretation), this experiment demonstrated that

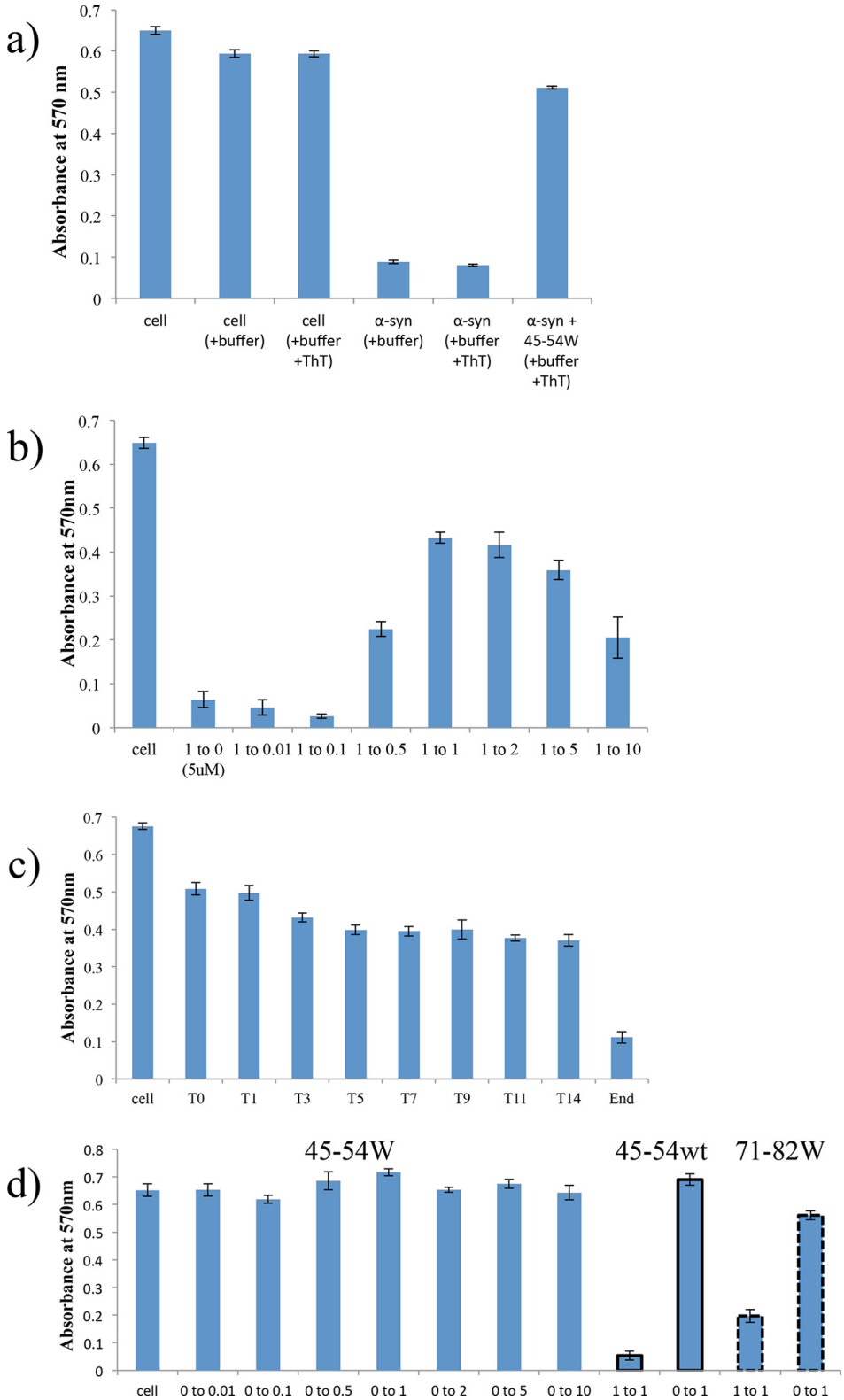

FIGURE 5. **MTT cytotoxicity assays using rat pheochromocytoma (PC12) cells and α-syn and the inhibitory effect of peptide 45–54W on α-syn aggregation.** *a*, shown from left to right are PC12 cells only, PC12 cells plus buffer, PC12 cells plus buffer and ThT, PC12 cells plus α-syn (5 μM) in buffer, PC12 cells plus α-syn (5 μM) in buffer plus ThT, and α-syn with peptide 45–54W at a 1:1 stoichiometry. The latter led to a large restoration of activity (~85%). *b*, increasing α-syn/peptide 45–54W molar ratios demonstrates a dose dependence. Samples were taken from the end point of the continuous growth experiment (75 h) and show that no effect on toxicity was observed at 1:0.01 or 1:0.1 and that a molar ratio of 1:0.5 was needed to partially rescue the cells (~28% recovery) from the cytotoxic effect of α-syn. This increased at 1:1 (~63%) and became progressively less pronounced at increasingly higher molar ratios. *c*, effect of incubation time on toxicity using samples taken directly from the continuous growth experiment. Results demonstrate that toxicity progressively increased as the sample aged and was at its maximum in the stationary phase of continuous growth. *d*, increasing concentrations of peptide 45–54W demonstrate that the peptide in isolation was not toxic to PC12 cells. MTT experiments using wild-type 45–54 sequence or peptide 71–82W demonstrate that the peptide was not toxic in isolation but at a ratio of 1:1 with α-syn had almost no effect upon toxicity. All experiments were undertaken in triplicate, and errors are shown as S.D.

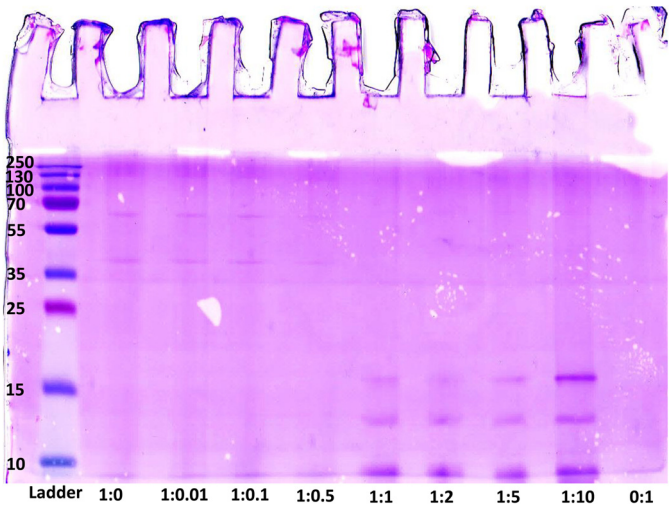

FIGURE 6. **SDS-PAGE analysis shows a range of samples taken from the end point (75 h) of continuous growth experiments.** Two clear bands at ~40 and ~60 kDa (as determined by graph analysis of log molecular mass *versus* relative migration distance) are present in the 1:0 sample, as well as in the 1:0.01, 1:0.1, 1:2, and 1:5 samples, suggesting the presence of α-syn trimers (40/14.5 = 2.8) and tetramers (60/14.5 = 4.1). At molar ratios of 1:1 or higher, these bands were absent and were replaced with three low molecular mass bands. One band at ~15 kDa may represent the α-syn·peptide 45–54W complex. The second and third bands are below the resolution limit of the gel but are likely to represent monomeric α-syn (14.5 kDa) and the inhibitor alone (1 kDa).

peptide 45–54W was able to interact with α-syn and lower the oligomeric state, possibly to the monomer.

DISCUSSION

In conclusion, we employed a semirational design combined with intracellular PCA to demonstrate this as an effective methodology for developing α-syn aggregation antagonists. To date, the majority of β-sheet breaker compounds either are designed to target or are based specifically on region 71–82 of the protein because it is known to aggregate in isolation and therefore thought to be responsible for instigating amyloidosis of the parent protein. Inhibitors include *N*-methylated derivatives of the same sequence (9), single-chain antibodies (31), and small-molecule compounds such as curcumin (32) and epigallocatechin gallate (33).

In contrast, our approach has focused on the development of a library centered on sequence 45–54, in which four of the five known α-syn familial mutants implicated in early-onset PD are found. All of the known mutations in this region result in either increased α-syn aggregation rates or increased numbers of oligomers and therefore increased levels of toxicity. All residues in sequence 45–54 were therefore scrambled to give two, three, or six options, giving rise to a library of 209,952 members (Fig. 1). This was constructed to include all wild-type options and the mutations found in E46K, A53T, and H50Q, respectively. Half of the 10 positions reselected the wild-type residues, whereas the remaining five resulted in new selections. These were E46D, V48I, H50N, A53K, and T54A. In amyloid inhibition experiments (*i.e.* inhibitor and monomeric α-syn mixed at time 0 and amyloid growth continuously monitored) and at a stoichiometry of 1:1, we observed that the classical sigmoidal amyloid growth for an inhibitor-free (1:0) sample was abolished. Instead, the signal was held at ~8% of the signal observed in the stationary phase of the 1:0 sample. At a stoichiometry of 1:0.5, amyloid growth was significantly slower, taking approximately twice as long for the fluorescence intensity to match that of the 1:0 sample. In accordance with an expected dose dependence, at a 1:0.1 stoichiometry or lower, the inhibitory effect was lost. The impressive efficacy of the 1:1 sample in continuous growth ThT experiments is supported by both CD data, which show that the conversion from a random coil-like structure consistent with native α-syn to a classical amyloid β-sheet signal did not occur in the 1:1 sample, and MTT data, which show that toxicity associated with α-syn aggregation was almost completely reversed in the presence of peptide 45–54W. Moreover, a clear reduction to almost no fibrils was observed by direct AFM imaging. This was corroborated by SDS-PAGE experiments showing the loss of low molecular mass oligomers in the presence of peptide 45–54W at a 1:1 stoichiometry or higher.

We have designed a library based on sequence 45–54 of wild-type α-syn and have created a potent peptide inhibitor of aggregation. In the future, it may be possible to derive more potent inhibitors of the mutagenic versions of α-syn that are in turn more effective with the wild-type protein. Not only does this point toward a new target for the design of new inhibitors, the peptide derived here using PCA has the potential itself to be modified into drugs to slow or even prevent the onset of PD.

Acknowledgments—We acknowledge use of the Park Systems XE-120 atomic force microscope, which was on loan from the Engineering and Physical Sciences Research Council Engineering Instrument Pool. We thank Dr. Miao Yu for excellent technical support.

REFERENCES

1. Fink, A. L. (2006) The aggregation and fibrillation of α-synuclein. *Acc. Chem. Res.* **39,** 628–634
2. Cookson, M. R. (2009) α-Synuclein and neuronal cell death. *Mol. Neurodegener.* **4,** 9
3. Irvine, G. B., El-Agnaf, O. M., Shankar, G. M., and Walsh, D. M. (2008) Protein aggregation in the brain: the molecular basis for Alzheimer's and Parkinson's diseases. *Mol. Med.* **14,** 451–464
4. Outeiro, T. F., Putcha, P., Tetzlaff, J. E., Spoelgen, R., Koker, M., Carvalho, F., Hyman, B. T., and McLean, P. J. (2008) Formation of toxic oligomeric α-synuclein species in living cells. *PLoS ONE* **3,** e1867
5. Giasson, B. I., Murray, I. V., Trojanowski, J. Q., and Lee, V. M. (2001) A hydrophobic stretch of 12 amino acid residues in the middle of α-synuclein is essential for filament assembly. *J. Biol. Chem.* **276,** 2380–2386
6. Madine, J., Doig, A. J., Kitmitto, A., and Middleton, D. A. (2005) Studies of the aggregation of an amyloidogenic α-synuclein peptide fragment. *Biochem. Soc. Trans.* **33,** 1113–1115
7. Periquet, M., Fulga, T., Myllykangas, L., Schlossmacher, M. G., and Feany, M. B. (2007) Aggregated α-synuclein mediates dopaminergic neurotoxicity *in vivo*. *J. Neurosci.* **27,** 3338–3346
8. El-Agnaf, O. M., Paleologou, K. E., Greer, B., Abogrein, A. M., King, J. E., Salem, S. A., Fullwood, N. J., Benson, F. E., Hewitt, R., Ford, K. J., Martin, F. L., Harriott, P., Cookson, M. R., and Allsop, D. (2004) A strategy for designing inhibitors of α-synuclein aggregation and toxicity as a novel treatment for Parkinson's disease and related disorders. *FASEB J.* **18,** 1315–1317
9. Madine, J., Doig, A. J., and Middleton, D. A. (2008) Design of an *N*-methylated peptide inhibitor of α-synuclein aggregation guided by solid-state NMR. *J. Am. Chem. Soc.* **130,** 7873–7881
10. Lesage, S., Anheim, M., Letournel, F., Bousset, L., Honoré, A., Rozas, N., Pieri, L., Madiona, K., Dürr, A., Melki, R., Verny, C., Brice, A., and French

Parkinson's Disease Genetics Study Group (2013) G51D α-synuclein mutation causes a novel parkinsonian-pyramidal syndrome. *Ann. Neurol.* **73,** 459–471
11. Bussell, R., Jr., and Eliezer, D. (2001) Residual structure and dynamics in Parkinson's disease-associated mutants of α-synuclein. *J. Biol. Chem.* **276,** 45996–46003
12. Greenbaum, E. A., Graves, C. L., Mishizen-Eberz, A. J., Lupoli, M. A., Lynch, D. R., Englander, S. W., Axelsen, P. H., and Giasson, B. I. (2005) The E46K mutation in α-synuclein increases amyloid fibril formation. *J. Biol. Chem.* **280,** 7800–7807
13. Ghosh, D., Mondal, M., Mohite, G. M., Singh, P. K., Ranjan, P., Anoop, A., Ghosh, S., Jha, N. N., Kumar, A., and Maji, S. K. (2013) The Parkinson's disease-associated H50Q mutation accelerates α-synuclein aggregation *in vitro*. *Biochemistry* **52,** 6925–6927
14. Rutherford, N. J., Moore, B. D., Golde, T. E., and Giasson, B. I. (2014) Divergent effects of the H50Q and G51D SNCA mutations on the aggregation of α-synuclein. *J. Neurochem.* **131,** 859–867
15. Pelletier, J. N., Campbell-Valois, F. X., and Michnick, S. W. (1998) Oligomerization domain-directed reassembly of active dihydrofolate reductase from rationally designed fragments. *Proc. Natl. Acad. Sci. U.S.A.* **95,** 12141–12146
16. Mason, J. M., Schmitz, M. A., Müller, K. M., and Arndt, K. M. (2006) Semirational design of Jun-Fos coiled coils with increased affinity: universal implications for leucine zipper prediction and design. *Proc. Natl. Acad. Sci. U.S.A.* **103,** 8989–8994
17. Acerra, N., Kad, N. M., Cheruvara, H., and Mason, J. M. (2014) Intracellular selection of peptide inhibitors that target disulphide-bridged Aβ42 oligomers. *Protein Sci.* **23,** 1262–1274
18. Acerra, N., Kad, N. M., and Mason, J. M. (2013) Combining intracellular selection with protein-fragment complementation to derive Aβ interacting peptides. *Protein Eng. Des. Sel.* **26,** 463–470
19. Butt, T. R., Edavettal, S. C., Hall, J. P., and Mattern, M. R. (2005) SUMO fusion technology for difficult-to-express proteins. *Protein Expr. Purif.* **43,** 1–9
20. Fields, G. B., and Noble, R. L. (1990) Solid-phase peptide synthesis utilizing 9-fluorenylmethoxycarbonyl amino acids. *Int. J. Pept. Protein Res.* **35,** 161–214
21. Maurer-Stroh, S., Debulpaep, M., Kuemmerer, N., Lopez de la Paz, M., Martins, I. C., Reumers, J., Morris, K. L., Copland, A., Serpell, L., Serrano, L., Schymkowitz, J. W., and Rousseau, F. (2010) Exploring the sequence determinants of amyloid structure using position-specific scoring matrices. *Nat. Methods* **7,** 237–242
22. Frousios, K. K., Iconomidou, V. A., Karletidi, C. M., and Hamodrakas, S. J. (2009) Amyloidogenic determinants are usually not buried. *BMC Struct. Biol.* **9,** 44
23. Trovato, A., Seno, F., and Tosatto, S. C. (2007) The PASTA server for protein aggregation prediction. *Protein Eng. Des. Sel.* **20,** 521–523
24. Tartaglia, G. G., and Vendruscolo, M. (2008) The Zyggregator method for predicting protein aggregation propensities. *Chem. Soc. Rev.* **37,** 1395–1401
25. Fernandez-Escamilla, A. M., Rousseau, F., Schymkowitz, J., and Serrano, L. (2004) Prediction of sequence-dependent and mutational effects on the aggregation of peptides and proteins. *Nat. Biotechnol.* **22,** 1302–1306
26. Kad, N. M., Myers, S. L., Smith, D. P., Smith, D. A., Radford, S. E., and Thomson, N. H. (2003) Hierarchical assembly of β_2-microglobulin amyloid *in vitro* revealed by atomic force microscopy. *J. Mol. Biol.* **330,** 785–797
27. Shearman, M. S., Ragan, C. I., and Iversen, L. L. (1994) Inhibition of PC12 cell redox activity is a specific, early indicator of the mechanism of β-amyloid-mediated cell death. *Proc. Natl. Acad. Sci. U.S.A.* **91,** 1470–1474
28. Hughes, E., Burke, R. M., and Doig, A. J. (2000) Inhibition of toxicity in the β-amyloid peptide fragment β-(25–35) using *N*-methylated derivatives: a general strategy to prevent amyloid formation. *J. Biol. Chem.* **275,** 25109–25115
29. Pike, C. J., Walencewicz-Wasserman, A. J., Kosmoski, J., Cribbs, D. H., Glabe, C. G., and Cotman, C. W. (1995) Structure-activity analyses of β-amyloid peptides: contributions of the β25–35 region to aggregation and neurotoxicity. *J. Neurochem.* **64,** 253–265
30. Hung, L. W., Ciccotosto, G. D., Giannakis, E., Tew, D. J., Perez, K., Masters, C. L., Cappai, R., Wade, J. D., and Barnham, K. J. (2008) Amyloid-β peptide (Aβ) neurotoxicity is modulated by the rate of peptide aggregation: Aβ dimers and trimers correlate with neurotoxicity. *J. Neurosci.* **28,** 11950–11958
31. Emadi, S., Liu, R., Yuan, B., Schulz, P., McAllister, C., Lyubchenko, Y., Messer, A., and Sierks, M. R. (2004) Inhibiting aggregation of α-synuclein with human single chain antibody fragments. *Biochemistry* **43,** 2871–2878
32. Singh, P. K., Kotia, V., Ghosh, D., Mohite, G. M., Kumar, A., and Maji, S. K. (2013) Curcumin modulates α-synuclein aggregation and toxicity. *ACS Chem. Neurosci.* **4,** 393–407
33. Bieschke, J., Russ, J., Friedrich, R. P., Ehrnhoefer, D. E., Wobst, H., Neugebauer, K., and Wanker, E. E. (2010) EGCG remodels mature α-synuclein and amyloid-β fibrils and reduces cellular toxicity. *Proc. Natl. Acad. Sci. U.S.A.* **107,** 7710–7715

Protein Structure and Folding:

Intracellular Screening of a Peptide Library to Derive a Potent Peptide Inhibitor of α-Synuclein Aggregation

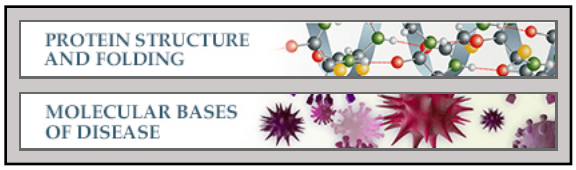

Harish Cheruvara, Victoria L. Allen-Baume, Neil M. Kad and Jody M. Mason

J. Biol. Chem. 2015, 290:7426-7435.
doi: 10.1074/jbc.M114.620484 originally published online January 23, 2015
